BLED WORKSHOPS
IN PHYSICS
VOL. 12, NO. 1
p. 18

Proceedings of the Mini-Workshop
Understanding hadronic spectra
Bled, Slovenia, July 3 - 10, 2011

Transversity structure of the pion in chiral quark models*

W. Broniowski[a,b], E. Ruiz Arriola[c,d], A. E. Dorokhov[e,f]

[a] Institute of Nuclear Physics PAN, PL-31342 Cracow, Poland
[b] Institute of Physics, Jan Kochanowski University PL-25406 Kielce, Poland
[c] Departamento de Física Atómica, Molecular y Nuclear, Universidad de Granada, E-18071 Granada, Spain
[d] Instituto Carlos I de Fisica Teórica y Computacional, Universidad de Granada E-18071 Granada, Spain
[e] Joint Institute for Nuclear Research, Bogoliubov Laboratory of Theoretical Physics RU-141980 Dubna, Russia
[f] Institute for Theoretical Problems of Microphysics, Moscow State University RU-119899 Moscow, Russia

Abstract. We describe the chiral quark model evaluation of the transversity Generalized Parton Distributions (tGPDs) and related transversity form factors (tFFs) of the pion. The obtained tGPDs satisfy all necessary formal requirements, such as the proper support, normalization, and polynomiality. The lowest tFFs, after the necessary QCD evolution, compare favorably to the recent lattice QCD determination. Thus the transversity observables of the pion support once again the fact that the spontaneously broken chiral symmetry governs the structure of the Goldstone pion. The proper QCD evolution is crucial in these studies.

This talk is based on our two recent works [1, 2], where more details and a complete list of references may be found. Its topic concerns the transversity Generalized Parton Distribution (tGPD) of the pion, the least-known of the Generalized Parton Distributions (see [3–5] and references therein for an extensive review). The definition involves aligned parton-helicity operators (maximum-helicity case). For the case of spin-0 hadrons, tGPDs arise because of the nonzero orbital angular momentum between the initial and final state, thus allowing to study the spin structure without the inherent complications of the explicit spin degrees of freedom, as in the case of the nucleon. In that situation the analysis of the spin structure of the pion is particularly appealing, however, the quantity will be very difficult to access experimentally.

A few years ago, however, lattice simulations [6] provided the lowest-order pion quark transversity form factors (tFFs), defined as Mellin moments of tGPDs

* Talk delivered by W. Broniowski

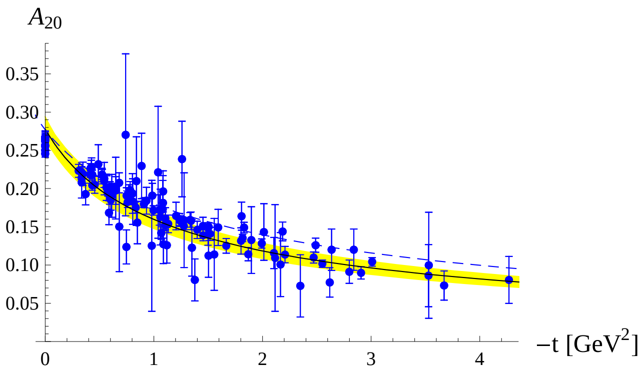

Fig. 1. The quark part of the spin-2 gravitational form factor in Spectral Quark Model (solid line) and NJL model with the Pauli-Villars regularization (dashed line), compared to the lattice data from Ref. [7,8]. The band around the Spectral Quark Model results corresponds to the model parameter uncertainty.

in the Bjorken x variable. That way lattices supply valuable information on the nontrivial spin structure of hadrons. In general, lattice calculations are capable to determine quantities that may only be dreamed off to be measured experimentally and, in that regard, are extremely useful. The results can be used to verify various theoretical approaches and models in their rich spectrum of predictions. An example is the gravitational form factor of the pion. Its lattice determination [7, 8] agrees remarkably well with the evaluation in chiral quark models [9], as can be seen from Fig. 1.

Our study consist of two distinct parts: 1) the chiral quark model determination of tFFs and tGPDs of the pion and 2) the QCD evolution. For the first part we apply the standard *local* NJL model with the Pauli-Villars regularization [10] and two versions of the *nonlocal* models, where the quark mass depends on the momentum of the quark, namely, the instanton model [11] and the Holdom-Terning-Verbeek (HTV) model [12]. We stress that chiral quark models have been successfully used for the evaluation of *soft* matrix elements entering numerous high-energy processes [9, 13–40]. They also agree with the Euclidean lattice determination of moments (see, e.g., [41, 42]) and direct results from the transverse lattices [43–46].

The second element, crucial in obtaining proper results, is the QCD evolution, where renorm-improved radiative gluonic corrections are appended. The method is schematically depicted in Fig. 2. One-loop (large-N_c) quark diagram, with external gauge bosons and Goldstone mesons, is evaluated. Then the renorm-improved gluon exchanges are incorporated in terms of the LO DGLAP evolution. The scale where the quark model calculation is carried out can be identified with the help of the momentum fraction carried by the quarks. According to phenomenology [47, 48] or lattice calculations [49], the valence quark contribution is 47% of the total at the scale $\mu = 2$GeV. Since the quark models possess no explicit gluons, the valence quarks carry 100% of the momentum. This determines the quark model scale, denoted as μ_0, as the scale determined in such a way, that

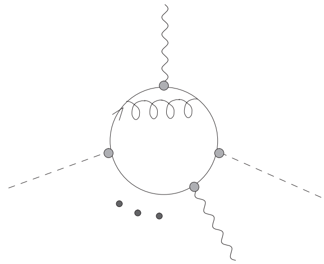

Fig. 2. One-loop (large-N_c) quark diagram, with external gauge bosons (wavy lines) and Goldstone mesons (dashed lines). The renorm-improved gluon exchanges are incorporated in terms of the LO DGLAP evolution.

when the evolution is carried out from μ_0 up to $\mu = 2$ GeV, the fraction drops to $47 \pm 2\%$. The result of the LO DGLAP evolution is

$$\mu_0 = 313^{+20}_{-10}\ \text{MeV}. \tag{1}$$

Despite the low value of this scale, the prescription has been successfully confirmed by a variety of high-energy data and lattice calculations (see [26] and references therein). Moreover, the NLO DGLAP modifications yield moderate corrections [14], supporting our somewhat strained use of perturbative QCD at low scales. To summarize, *our approach = chiral quark model + QCD evolution*.

We now come to definitions. The pion u-quark tFFs, denoted as $B^{\pi,u}_{ni}(t)$, are defined via [50]

$$\langle \pi^+(p')|\overline{u}(0) i\sigma^{\mu\nu} a_\mu b_\nu \left(i \overleftrightarrow{D} a\right)^{n-1} u(0)|\pi^+(p)\rangle = (a\cdot P)^{n-1} \frac{[a\cdot p\, b\cdot p']}{m_\pi} \times \sum_{\substack{i=0,\\ \text{even}}}^{n-1} (2\xi)^i B^{\pi,u}_{ni}(t)\,, \tag{2}$$

where the auxiliary vectors a and b satisfy the conditions $a^2 = (ab) = 0$ and $b^2 \neq 0$. The skewness parameter is defined as $\xi = -a\cdot q/(2a\cdot P)$, the symbol $\overleftrightarrow{D}^\beta = \overleftrightarrow{\partial}^\beta - igA^\beta$ is the covariant derivative, and $\overleftrightarrow{\partial}^\beta = \frac{1}{2}\left(\overrightarrow{\partial}^\beta - \overleftarrow{\partial}^\beta\right)$. Next, p' and p are the initial and final pion momenta, $P = \frac{1}{2}(p'+p)$, $q = p'-p$, and $t = -q^2$. The bracket denotes antisymmetrization in the vectors a and b. The corresponding definition of the tGPD is [3]

$$\langle \pi^+(p') \mid \bar{u}(-a) i\sigma^{\mu\nu} a_\mu b_\nu u(a) \mid \pi^+(p)\rangle = \frac{[a\cdot p\, b\cdot p']}{m_\pi} \int_{-1}^{1} dx\, e^{-ix\,P\cdot a} E^{\pi,u}_T(x,\xi,t), \tag{3}$$

where the presence of the gauge link operator are understood. The tFFs for the d-quarks follow from the isospin symmetry, namely $B^{\pi,d}_{ni}(t) = (-1)^n B^{\pi,u}_{ni}(t)$. The tFFs are the moments of the tGPD in the x-variable,

$$\int_{-1}^{1} dx\, x^{n-1} E^{\pi,u}_T(x,\xi,t) = \sum_{\substack{i=0,\\ \text{even}}}^{n-1} (2\xi)^i B^{\pi,u}_{ni}(t)\,. \tag{4}$$

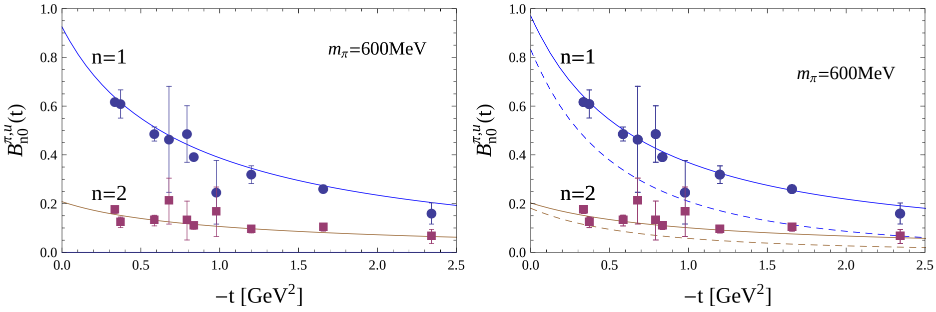

Fig. 3. The form factors $B^{\pi,u}_{10}(t)$ and $B^{\pi,u}_{20}(t)$, evaluated at $m_\pi = 600$MeV in the local NJL model (left panel) and in nonlocal models (right panel, solid line – HTV model, dashed line – instanton model). The lattice data from [6]. The local NJL and HTV models agree very well with the data.

This formula explicitly displays the desired polynomiality property. We remark that the full information carried by tGPDs is contained in the collection of the infinitely many tFFs.

The full details of the quark-model calculation as well as the QCD evolution can be found in [1,2]. The two lowest tFFs available from the lattice data, $B^{\pi,u}_{10}$ and $B^{\pi,u}_{20}$, evolve multiplicatively in a simple way:

$$B^{\pi,u}_{n0}(t;\mu) = B^{\pi,u}_{n0}(t;\mu_0)\left(\frac{\alpha(\mu)}{\alpha(\mu_0)}\right)^{\gamma^T_n/(2\beta_0)}, \tag{5}$$

where γ^T_n are the appropriate anomalous dimensions [1,2]. In the local model, in the chiral limit at $t = 0$ we find the very simple result:

$$B^{\pi,u}_{10}(t=0;\mu_0)/m_\pi = \frac{N_c M}{4\pi^2 f_\pi^2}, \quad \frac{B^{\pi,u}_{20}(t=0;\mu)}{B^{\pi,u}_{10}(t=0;\mu)} = \frac{1}{3}\left(\frac{\alpha(\mu)}{\alpha(\mu_0)}\right)^{8/27}, \tag{6}$$

where M is the constituent quark mass. The results of the model calculation followed by evolution are shown in Fig. 3. We note a striking agreement with the lattice data [6] for the local NJL model, as well as for the non-local HTV model.

Finally, we present the results for the full tGPD for $t = 0$ and $\xi = 1/3$ or $\xi = 0$. The evolution is different for the symmetric and antisymmetric parts of tGPDs, hence we define the isovector and isoscalar combinations:

$$E^{\pi,I=1}_T(x,\xi,Q^2) \equiv E^{\pi,S}_T(x,\xi,Q^2) = E^\pi_T(x,\xi,Q^2) + E^\pi_T(-x,\xi,Q^2),$$
$$E^{\pi,I=0}_T(x,\xi,Q^2) \equiv E^{\pi,A}_T(x,\xi,Q^2) = E^\pi_T(x,\xi,Q^2) - E^\pi_T(-x,\xi,Q^2).$$

The QCD evolution has been carried out with the method of [51–54]. The results for $\xi = 1/3$ in the NJL model are shown in Fig. 4, while in Fig. 5 we compare the result for $\xi = 0$ in the NJL model (left panel) and the nonlocal instanton model (right panel). Except for different end-point behavior, discussed in [2], the results are similar.

In conclusion we wish to stress that the absolute predictions for the multiplicatively evolved B_{10} and B_{20} agree remarkably well with the lattice results,

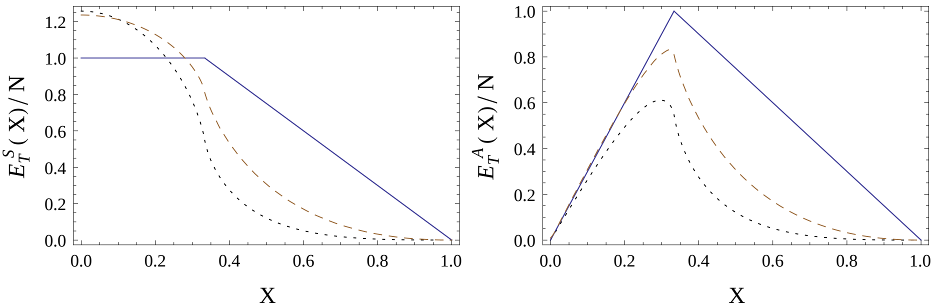

Fig. 4. The symmetric (left panel) and antisymmetric (right panel) tGPDs of the pion at $t = 0$ and $\xi = 1/3$, evaluated in the NJL model in the chiral limit at the quark-model scale $\mu_0 = 313$ MeV (solid lines) and evolved to the scales $\mu = 2$ GeV (dashed lines) and 1 TeV (dotted lines).

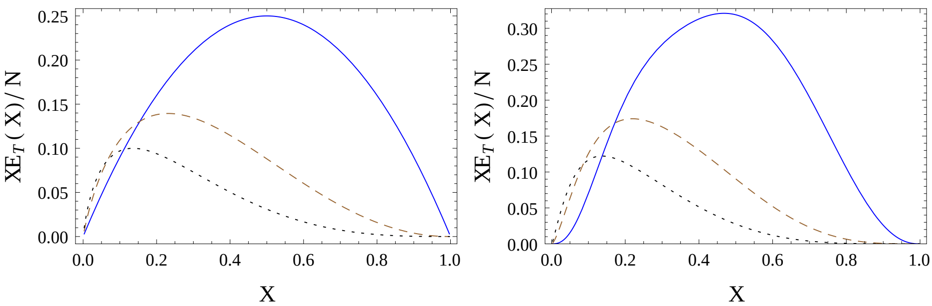

Fig. 5. The tGPD of the pion at $t = 0$ and $\xi = 0$, evaluated in the chiral limit in the local NJL model (left panel) and in the instanton model (right panel). The solid lines correspond to the quark-model scale $\mu_0 = 313$ MeV, the dashed lines to $\mu = 2$ GeV, and the dotted lines to $\mu = 1$ TeV.

supporting the assumptions of numerous other calculations following the same "chiral quark model + QCD evolution" scheme. Our study of the transversity observables of the pion support once again the feature that the spontaneously broken chiral symmetry determines the structure of the Goldstone pion.

Acknowledgments This work is supported by the Bogoliubov-Infeld program (JINR), the Polish Ministry of Science and Higher Education, grants N N202 263438 and N N202 249235, Spanish DGI and FEDER grant FIS2008-01143/FIS, Junta de Andalucía grant FQM225-05, and EU Integrated Infrastructure Initiative Hadron Physics Project, contract RII3-CT-2004-506078. AED acknowledges partial support from the Russian Foundation for Basic Research, projects No. 10-02-00368 and No. 11-02-00112.

References

1. W. Broniowski, A.E. Dorokhov and E.R. Arriola, Phys. Rev. D82 (2010) 094001, 1007.4960.

2. A.E. Dorokhov, W. Broniowski and E.R. Arriola, Phys. Rev. D 84 (2011) 074015, 1107.5631.
3. A.V. Belitsky and A.V. Radyushkin, Phys. Rept. 418 (2005) 1, hep-ph/0504030.
4. T. Feldmann, Eur. Phys. J. Special Topics 140 (2007) 135.
5. S. Boffi and B. Pasquini, Riv. Nuovo Cim. 30 (2007) 387, 0711.2625.
6. QCDSF, D. Brommel et al., Phys. Rev. Lett. 101 (2008) 122001, 0708.2249.
7. D. Brommel et al., PoS LAT2005 (2006) 360, hep-lat/0509133.
8. D. Brommel, Pion structure from the lattice, PhD thesis, University of Regensburg, Regensburg, Germany, 2007, DESY-THESIS-2007-023.
9. W. Broniowski and E.R. Arriola, Phys.Rev. D78 (2008) 094011, 0809.1744.
10. E. Ruiz Arriola, Phys. Lett. B253 (1991) 430.
11. D. Diakonov and V.Y. Petrov, Nucl. Phys. B272 (1986) 457.
12. B. Holdom, J. Terning and K. Verbeek, Phys. Lett. B245 (1990) 612.
13. R.M. Davidson and E. Ruiz Arriola, Phys. Lett. B348 (1995) 163.
14. R.M. Davidson and E. Ruiz Arriola, Acta Phys. Polon. B33 (2002) 1791, hep-ph/0110291.
15. W. Broniowski and E. Ruiz Arriola, Phys. Lett. B574 (2003) 57, hep-ph/0307198.
16. A.E. Dorokhov and L. Tomio, (1998), hep-ph/9803329.
17. M.V. Polyakov and C. Weiss, Phys. Rev. D60 (1999) 114017, hep-ph/9902451.
18. A.E. Dorokhov and L. Tomio, Phys. Rev. D62 (2000) 014016.
19. I.V. Anikin et al., Nucl. Phys. A678 (2000) 175.
20. M. Praszalowicz and A. Rostworowski, Acta Phys. Polon. B34 (2003) 2699, hep-ph/0302269.
21. A. Bzdak and M. Praszalowicz, Acta Phys. Polon. B34 (2003) 3401, hep-ph/0305217.
22. T. Nguyen et al., Phys. Rev. C83 (2011) 062201, 1102.2448.
23. L. Theussl, S. Noguera and V. Vento, Eur. Phys. J. A20 (2004) 483, nucl-th/0211036.
24. F. Bissey et al., Phys. Lett. B587 (2004) 189, hep-ph/0310184.
25. S. Noguera and V. Vento, Eur. Phys. J. A28 (2006) 227, hep-ph/0505102.
26. W. Broniowski, E. Ruiz Arriola and K. Golec-Biernat, Phys. Rev. D77 (2008) 034023, 0712.1012.
27. T. Frederico et al., Nucl. Phys. B (Proc. Supp.) 199 (2010) 264, 0911.1736.
28. T. Frederico et al., Phys. Rev. D80 (2009) 054021, 0907.5566.
29. S.V. Esaibegian and S.N. Tamarian, Sov. J. Nucl. Phys. 51 (1990) 310.
30. A.E. Dorokhov, Nuovo Cim. A109 (1996) 391.
31. V.Y. Petrov et al., Phys. Rev. D59 (1999) 114018, hep-ph/9807229.
32. I.V. Anikin, A.E. Dorokhov and L. Tomio, Phys. Lett. B475 (2000) 361, hep-ph/9909368.
33. M. Praszalowicz and A. Rostworowski, Phys. Rev. D64 (2001) 074003, hep-ph/0105188.
34. A.E. Dorokhov, JETP Lett. 77 (2003) 63, hep-ph/0212156.
35. E. Ruiz Arriola and W. Broniowski, Phys. Rev. D66 (2002) 094016, hep-ph/0207266.
36. E. Ruiz Arriola, Acta Phys. Polon. B33 (2002) 4443, hep-ph/0210007.
37. B.C. Tiburzi, Phys. Rev. D72 (2005) 094001, hep-ph/0508112.
38. W. Broniowski and E. Ruiz Arriola, Phys. Lett. B649 (2007) 49, hep-ph/0701243.
39. A. Courtoy and S. Noguera, Prog. Part. Nucl. Phys. 61 (2008) 170, 0803.3524.
40. P. Kotko and M. Praszalowicz, Acta Phys. Polon. B40 (2009) 123, 0803.2847.
41. B.U. Musch et al., Phys. Rev. D83 (2011) 094507, 1011.1213.
42. P. Hagler, Phys. Rept. 490 (2010) 49, 0912.5483.
43. M. Burkardt and S. Dalley, Prog. Part. Nucl. Phys. 48 (2002) 317, hep-ph/0112007.
44. S. Dalley, Phys. Rev. D64 (2001) 036006, hep-ph/0101318.
45. S. Dalley, Few Body Syst. 36 (2005) 69, hep-ph/0409139.
46. S. Dalley and B. van de Sande, Phys. Rev. D67 (2003) 114507, hep-ph/0212086.

47. P.J. Sutton et al., Phys. Rev. D45 (1992) 2349.
48. M. Gluck, E. Reya and I. Schienbein, Eur. Phys. J. C10 (1999) 313, hep-ph/9903288.
49. C. Best et al., Phys. Rev. D56 (1997) 2743, hep-lat/9703014.
50. M. Diehl and L. Szymanowski, Phys. Lett. B690 (2010) 149, 1003.4171.
51. N. Kivel and L. Mankiewicz, Phys. Lett. B458 (1999) 338, hep-ph/9905342.
52. N. Kivel and L. Mankiewicz, Nucl. Phys. B557 (1999) 271, hep-ph/9903531.
53. A. Manashov, M. Kirch and A. Schafer, Phys. Rev. Lett. 95 (2005) 012002, hep-ph/0503109.
54. M. Kirch, A. Manashov and A. Schafer, Phys. Rev. D72 (2005) 114006, hep-ph/0509330.